Chapter 4
Stability Assessment of Markundi Hills Using Q-slope, SMR and Simulation Tools

Ashutosh Kainthola, Vishnu Himanshu Ratnam Pandey, P. K. Singh, and T. N. Singh

Abstract Stable roads in hilly regions are not only a boon for the economy but also contribute to betterment of human lives and infrastructure. However, safe and cost-effective excavation design for road construction is a challenge. Lithology, slope geometry, rock mass-discontinuity, hydrogeology, excavation methods, etc., possess an intense influence on stability of excavated hill slopes. There are numerous methods to assess and curtail the instability, from conventional chart-based methods to cutting-edge numerical simulation techniques. Yet, all the techniques have their advantages and disadvantages. Thus, in order to conduct a holistic instability assessment, it becomes essential to use different assessment techniques in conjunction. In the present study, sandstone cut slopes of Markundi hills in the district of Sonbhadra, Uttar Pradesh (UP), India, have been examined to ascertain the instability attributes. The cut slopes were initially investigated through kinematic analysis in DIPS software and then geomechanical classification techniques, viz., Q-slope and Continuous-SMR. This assessment enabled us to designate the modes of structurally controlled failures and their extent. Afterward, the RocFall program was employed to verify and corroborate the results of the rockfall dynamic in the study area. The slopes in the Markundi region were found stable on a large scale; however, small-scale localized failures due to intersecting discontinuities were a pressing issue, discovered in the study and validated in the field. The study emphasizes the risks associated with the detached blocks lying on the road, while passing through the region. Also, slight flattening (1°–3°) of the slopes at all these studied sections may reduce the risk to a great extent.

Keywords Slope failure · Kinematic analysis · Q-slope · CSMR · Markundi ills

A. Kainthola · V. H. R. Pandey (✉)
Geo-Engineering & Computing Laboratory, Department of Geology, Banaras Hindu University, Varanasi 221005, India
e-mail: pandey.vhr@bhu.ac.in

P. K. Singh
Department of Earth and Planetary Sciences, University of Allahabad, Prayagraj 211002, India

T. N. Singh
Department of Civil and Environmental Engineering, Indian Institute of Technology, Patna 801106, Bihar, India

P. Thambidurai and T. N. Singh (eds.), *Landslides: Detection, Prediction and Monitoring*,
https://doi.org/10.1007/978-3-031-23859-8_4

4.1 Introduction

The ancient human civilizations settled mainly along river plains; however, alarming population growth forced them to shift towards hilly terrains in search of better habitable space (Petley et al. 2005; Deng et al. 2018). Mountains constitute an important segment of several countries, and numerous people make their living in these perilous landforms. Until the last century, there were no sophisticated means of commutable infrastructure in the mountainous regions. Hence, the hilly people remained unconnected with the rest of the world. With scientific advancement in the construction sector and government initiatives to bring these regions into the mainstream of the nation's growth, major civil and engineering projects were launched (Singh et al. 2010, 2013, 2017; Ray et al. 2020). Still, the challenges are quite big in implementing these construction works as the engineers and policymakers have to consider rugged topography, tectonic disturbances, seismic activities, disturbed geological setup, and frequent landslide and rainfall phenomena in the mountainous regions (Glade et al. 2000; Singh et al. 2018; Kundu et al. 2022).

The slope instability is the leading concern in fostering safe and economic highway projects in hilly regions. Therefore, a thorough comprehension of slope mass geotechnical and geological attributes is mandatory in planning these megaprojects (Dikshit et al. 2020). The inherent discontinuities present in the rock mass has good control over slope stability, and it can be comprehended through kinematic analysis (Yoon et al. 2002). Moreover, the availability of meteorological data pertaining to these construction areas can boost the safety concern of the slope's failures to a great extent by addressing the issue of pore water pressure (Glade 2003; Glade et al. 2006). Certain instances of glacial melting had been reported as a causal factor of these unfortunate events, owing to the flow of melted water in cracks, fractures, and pore spaces present in the slope mass (Kos et al. 2016). Based on their proximity to tectonic plate boundaries, one needs to check the pseudo-static and dynamic earthquake forces operating in the study area (Zhou et al. 2015). The chief causes of instability differ from one place to another; however, these aforementioned factors always need careful consideration. The gentler cut slopes are generally stable but are uneconomical, and working area constraints are also significant (Tiwari et al. 2020).

On the contrary, steeper slopes can be unstable (Mahanta et al. 2016), although cost-effective. The cut slopes, which possess overall stability, show localized failures, especially rockfalls (Castelli et al. 2021; Singh et al. 2016). Rockfalls signify the swift downward movement of a broken block of rock through rolling, bouncing, and falling (Castelli et al. 2009; Scavia et al. 2020; Wei et al. 2022). Therefore, a thorough investigation is necessary to ascertain the rock mass behaviour, as a function of slope geometry, rock mass strength, and hydrological and stress regime of the area (Ansari et al. 2021). The representative geometric and strength properties are further employed to discern the factor of safety of the slope, which is the ratio of resisting to driving forces acting on the failure surface (Kainthola et al. 2013).

Many new and existing road projects are being developed by the Indian government (Financial Express 2022). Better transportation will facilitate the timely transfer

of goods and services from one part of the nation to another and boost the country's economy. Road widening and construction in hilly regions pose a peculiar stability and safety challenge (Kainthola et al. 2021). Slope collapses, regardless of scale, are hazardous to the moving traffic and economy (Infante et al. 2019). Around 15% of the Indian territory is vulnerable to landslides (NDMA 2022). Often, the highway excavation is unscientific, with minimal consideration for the geotechnical, engineering, and geological attributes of the slope forming material. The analysis is further aggravated for rock masses which are discontinuous, in-homogeneous, anisotropic and non-elastic (Hudson and Harrison 2000). The analysis of rock slopes generally entails either the assessment of structural instability-limit equilibrium-numerical simulation (Prakash et al. 2015). However, all the stability analysis techniques are underpinned by certain assumptions. It is thus recommended to use different approaches for the investigation.

In the present research, a combination of Q-slope, Continuous Slope mass rating (CSMR), and rockfall simulation approaches have been used to discern the stability of Markundi hills (Sonbhadra, UP) in Northern India. The hills are intersected by a state highway, continuing the regions to different parts of India. Based on the primary field investigation, three locations were chosen for the present study.

4.2 Study Area

The study area is a part of the Son-Valley region, the eastern extension of the Vindhyan Supergroup. Vindhyan Supergroup is the ramification of sedimentary processes operated in the Proterozoic Eon without any major evidence of metamorphism or tectonic activity (Kumar et al. 2002). The earlier workers classified the Vindhyan sequence into two groups, namely, the Upper Vindhyan (Bhander—Rewa—Kaimur Groups) and the Lower Vindhyan (Semri Group) (Auden 1933). The sickle-shaped intracratonic basin is an approximately 4.3 km thick sequence of sandstone-limestone-shale, exposed to over the area of 105 km^2, the rest being masked by Deccan traps and Gangetic Plains (Krishnan and Swaminath 1959; Tripathy and Singh 2015). The system of Son-Narmada Fault encloses the sequence, the Monghyr-Saharsa Ridge, Great Boundary Fault in the south, east, and west, respectively, whereas in the north-side Bundelkhand Massif along with Indo-Gangetic Plain is its border (NDR 2022). The basin is assigned the status of largest as well as thickest sedimentary sequence across the planet.

The area of interest, Markundi, is located at an elevation of 318 m above sea level in the Sonbhadra district of Uttar Pradesh (India). It is 370 km (in the south-east) from the state capital Lucknow and 94 km (in the south) from the holy city of Varanasi. The village houses nearly 7,303 people who speak Hindi, and their literacy rate is 47.5% (Census of India 2011). The steep cliff-forming Markundi hill has been traversed by state highway-5 (SH-5). The SH-5 is quite busy and often poses difficulty in conducting slope investigations. The dominant rock type in the area are Dhandrual quartzite and Scarp sandstone, which belong to the Kaimur Group

of the Upper Vindhyan Supergroup (Mishra and Sen 2012; Quasim et al. 2019) as presented in Fig. 4.1, with the google earth image pointing the research sites, along the State Highway-5. The Dhandrual sandstone formations, found at the top of the Kaimur group, are dirty to pure white, arenaceous, and medium to coarse-grained; they are underlain by Scarp sandstone formations, which are variegated with medium grains (Mishra and Sen 2011). The Marklund-Jamual fault is also present in the lower part of the hill, separating the scarp sandstones from underlying basement rocks (Bhattacharya et al. 2008). The studied sections are composed of Dhandrual sandstones. These sandstone beds are tabular with high lateral continuity. Numerous sedimentary structures can be noticed, namely large-scale cross bedding, ripples marks, flute, load casts, and herringbone structures. The area (Sonbhadra district) receives an annual rainfall of 928.7 mm, most of which comes as monsoonal precipitation, i.e., 840.8 mm (Guhathakurta et al. 2020). A research-based on the annual rainfall and temperature data collection for 20 years demonstrates a trend of yearly rise in temperature and fall in precipitation (Kumar et al. 2020).

4.3 Methodology

Initially, the field investigation was conducted in the Markundi area to acquire structural and geological data, based on which suitable samples were brought to the laboratory to examine their strength parameters. The field and laboratory data facilitated the calculation of Q-slope and CSMR and rockfall simulation. The field investigation aimed to collect the geological-structural-geometrical-geotechnical data of the cut slopes. Recordings were taken of the discontinuity sets, roughness, persistence, continuity, and hydrological signatures. The structural orientations of geological discontinuities were measured by the Brunton compass and classified into different sets based on their direction and amount of dip. The readings of the joint roughness were ascertained by Barton comb, while persistence was taken using a measuring tape. Scanline survey was employed for the enumeration of rock quality designation (RQD) in the field, through the calculation of joint frequency. The representative RQD for the slope locations has been assessed through the Eqs. (4.1) and (4.2) proposed by Priest and Hudson (1976).

$$\mathrm{RQD} = 100e^{-0.1\lambda}(0.1\lambda + 1) \tag{4.1}$$

where λ is the discontinuity frequency. For λ in the range of 6–6 m^{-1}, a reliable estimate of the equation is:

$$\mathrm{RQD} = 110.4 - 3.68\lambda \tag{4.2}$$

Further, the representative samples of the Dhandraul sandstone were tested in the laboratory. Three locations were chosen for the assessment based on visual evidence of vulnerability and failure (Fig. 4.2a and b). The rock mass at each location was

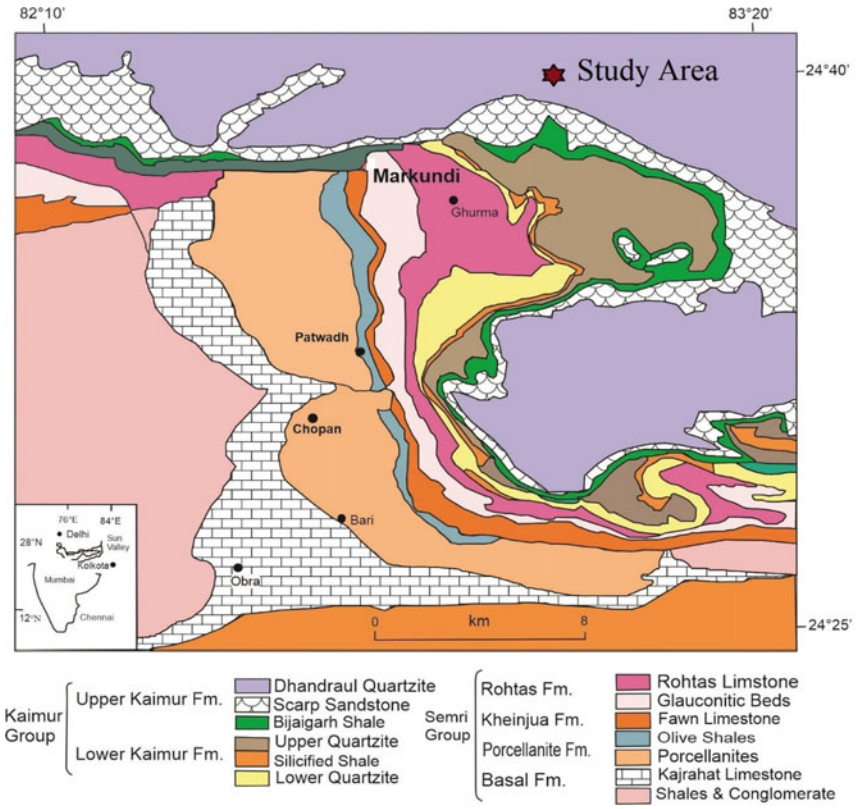

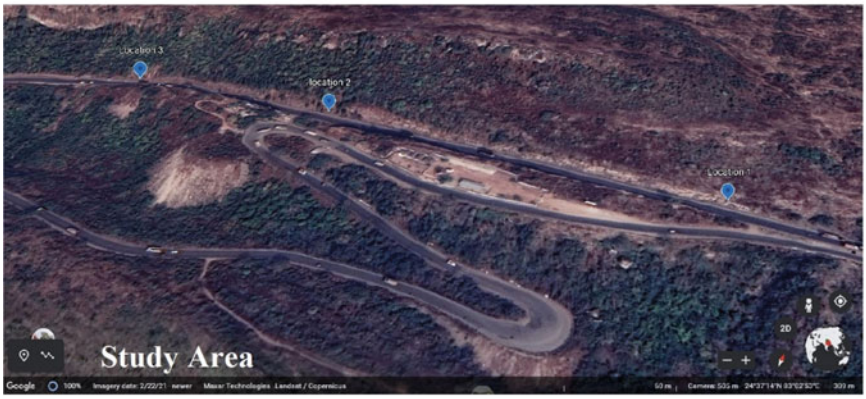

Fig. 4.1 Geological map of the study area (after Mishra and Sen 2012)

traversed by three sets of prominent joints. Failed rock blocks were also noticed along these chosen sections of the slope. Three prominent sets of discontinuities were marked in the field, as given in Table 4.1. The frequency of the joint sets was designated as J_1, J_2, and J_3, and the structural data was used to carry out a kinematic analysis. The DIPS software eases the identification of possible modes of failure (plane-wedge-topple) for each of these locations (Rocscience Inc. 2022). The analysis involves using stereographic projection of discontinuities in an equal area net to identify the blocks that permit movement (Basahel and Mitri 2017). This analysis considers the orientation of the discontinuity planes with respect to the slope face, plunge of intersecting discontinuities, and angle of internal friction along the joint plane. The kinematic examination was conditioned for planar, wedge, and toppling failures. The software needs inputs like structural discontinuities in the rock mass of the cut-slopes at each location combined with slope face orientation and angle of internal friction along these joint planes.

Additionally, the intact rock specimens were tested to discern their point load strength index (PLSI) (Fig. 4.3). Afterward, these index values were transformed

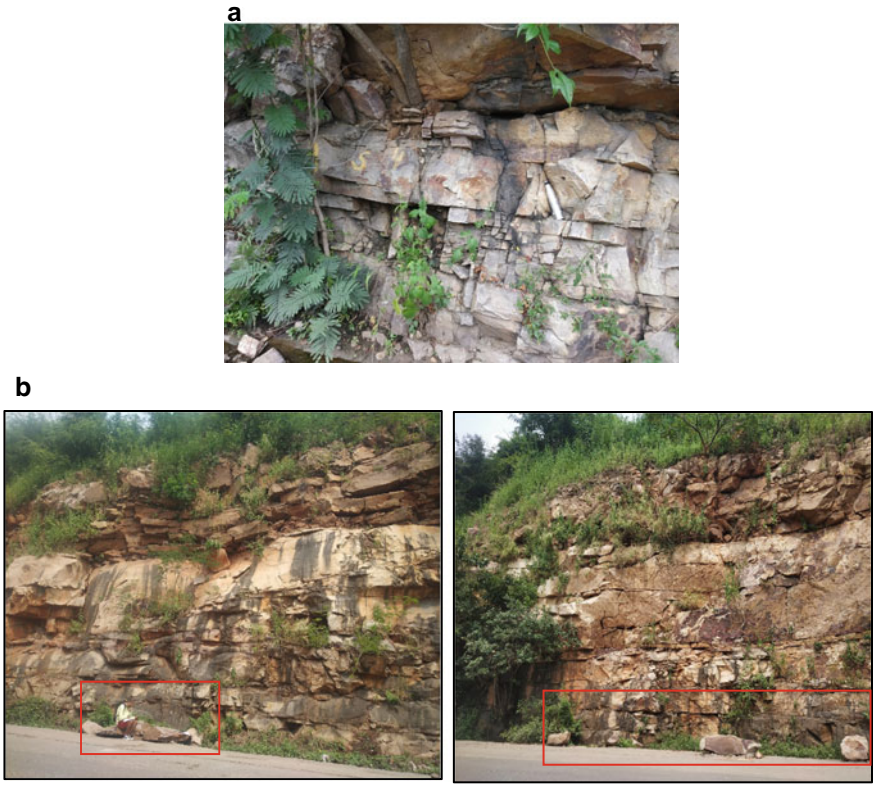

Fig. 4.2 **a** Rock mass condition at location 1, **b** Detached blocks lying on the road at locations 2 and 3 (in the red box)

Table 4.1 Structural orientation of the discontinuities in the rock mass along the studied sections

Locations	J_1		J_2		J_3		Slope	
	Dip Amount	Dip Direction	Dip Amount	Dip Direction	Dip Amount	Dip Direction	Angle	Aspect
1	20°	290	55°	110	60°	250	75°	190
2	05°	235	70°	110	80°	210	80°	180
3	70°	160	22°	030	78°	205	80°	190

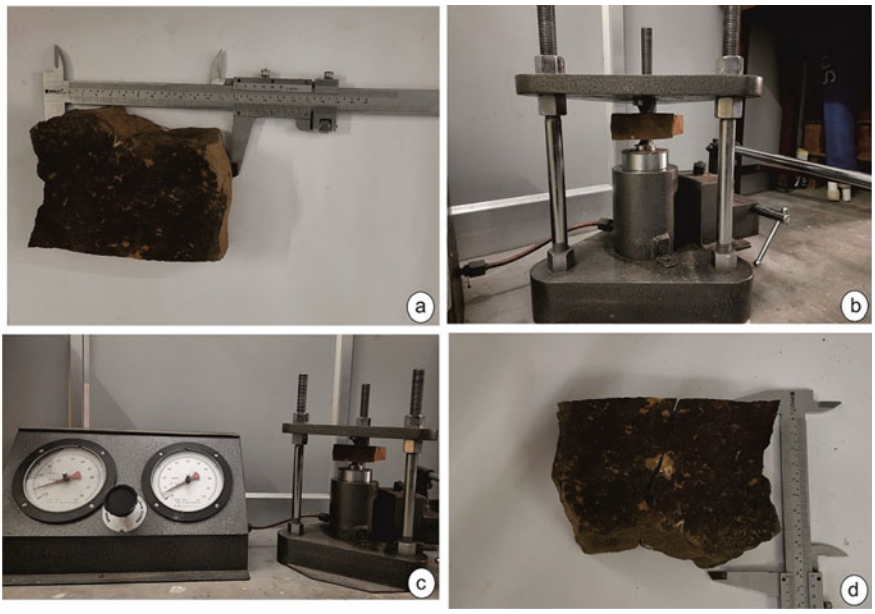

Fig. 4.3 Laboratory examination of rock sample for point load strength index (a) specimen's measurement before testing, (b) experimental setup, (c) experiment's data recording, and (d) broken rock sample after testing

into uniaxial compressive strength (UCS) using Eq. (4.3), mentioned in the literature. Previously, many researchers have recommended mathematical functions to translate PLSI values into uniaxial compressive strength (UCS) of rocks (Singh et al. 2012; Li and Wong 2013). These values were used for the geomechanical classification of the rock mass, basic-rock mass rating (RMRbasic), and further in the estimation of continuous slope mass rating (CSMR) and Q-Slope.

$$\mathrm{UCS} = k * \mathrm{PLSI} \tag{4.3}$$

where k ranges from 20 to 24. However, to comprehend the pragmatic rock mass scenario at the site and prevent the overestimation of UCS, 20 is assigned to k.

Finally, along with strength data, the rock mass of the slopes was classified, using Q-slope, $RMR_{basic,}$ and CSMR. In the evaluation of RMR_{basic} and CSMR, the authors have used open source QuickRMR software package (Kundu et al. 2020). Rock mass rating (RMR_{basic}) is a geomechanical classification scheme to designate the quality of the rock mass based on its UCS, RQD, joint spacing, groundwater condition, and discontinuity orientations (Bieniawski 1989). The first five parameters constitute RMR_{basic}, which is used to classify the rock mass, ignoring the joint orientation regarding the type of excavation/construction (Eq. 4.4).

$$RMR_{basic} = UCS + RQD + DS + DC + GW \tag{4.4}$$

where UCS corresponds to uniaxial compressive strength of the intact rock, RQD is rock quality designation, DS is spacing between the discontinuity, DC denotes the discontinuity condition, and GW stands for groundwater conditions.

The rock mass at the three locations has been ascribed with an RMR_{basic} value which has been further used to classify the slope, considering the corrections factor (adjustment rating). In the present work, continuous slope mass rating (CSMR) has been used to assess the stability of slopes. The CSMR is a modification to the earlier slope mass rating (SMR) scheme (Romana 1985). Measurement for discontinuity spacing, discontinuity condition, and groundwater attributes was made in the field investigation. Later ascertained values were used as input in the QuickRMR to calculate RMR_{basic} and then Continuous-SMR on applying adjustment rating factor owing to discontinuity orientations.

Q-slope is an excellent empirical approach for the quick estimation of safe slope angle for reinforcement free excavated slopes (Barton and Bar 2015). It takes inspiration from the Q-system designed especially for examining the rock-mass conditions in the tunnels and underground excavations in order to design suitable support system (Barton and Grimstad 2014). Similarly, one can devise a suitable mechanical stabilization or reinforcement needed for the slopes being excavated/examined or infer the maximum stable slope angle (without heavy support techniques) using the Q-slope method in the field itself. The basic structure of the Q-system remains the same in Q-slope, with few modifications in the existing parameters and the involvement of the orientation-factor (O-factor) in Eq. (4.5) (Bar and Barton 2017).

$$\text{Q-slope} = \left(\frac{RQD}{J_n}\right) * \left(\frac{J_r}{J_a} * \text{O-factor}\right) * \left(\frac{J_{wice}}{SRF_{slope}}\right) \tag{4.5}$$

where RQD, J_n, J_r, J_a, J_{wice}, SRF_{slope} are Rock Quality Designation, Joint set number, Joint roughness number, Joint alteration number, Geological and environmental condition of the excavated slope, and Strength reduction factors (a, b, and c) respectively. The maximum among the SRF_a, SRF_b, and SRF_c is always the best choice to correctly determine the steepest and most stable slope without any complicated support system. The steepness (β) of the unsupported safe slope can be determined using Eq. (4.6) (Singh et al. 2020) based on the determined Q-slope.

$$\beta = \left[20\log_{10}(\text{Q-slope}) + 65\right]^{\circ} \tag{4.6}$$

Eventually, rockfall analysis was done owing to the field evidence through the RocFall simulation package by Rocscience. The software calculates the energy and bounces height properties for each slope condition to comprehend the various conditions pertaining to rockfalls in the region. This information can be used to design mitigation measure in order to avert any future calamity. The mode of block movement (roll, bounce, fall) is a function of the slope steepness (Fig. 4.4); therefore, special consideration to slope angle should be given in rockfall studies. Apart from that, the shape and size of the rock-blocks plays a key role in deciding the rockfall trajectory. The slope roughness and effect of vegetation are critical factors that need to be assimilated in rockfall simulation programs to model block paths judiciously. As the greater the slope roughness, the higher the chances of divergence from original falling rock pieces. Also, the density of vegetation has a significant control on block movement, as it can either stop or deflect the natural path of the detached block from the source zone. However, in the present research owing to enormous slope steepness (75°–80°), "fall" will be the type of block movement. Therefore, the negligible collision between the slope surface and falling block will occur, and the effect of slope roughness can be neglected here. Additionally, the role of vegetation can also be ignored in the present work, as the hindrance offered by small trees and plants (on the basis ground-condition) can be ignored due to the slope's steepness and higher volume of falling blocks (~2 m^3).

For simulating the rockfall scenario at the three locations, a 2-D slope sections were designed to mimic the real slope geometry (based on determined slope angle and slope height as per field observation). The slope heights of 35 m, 32 m and 25 m were incorporated in the RocFall model, while slope angles were 75°, 80°, and 80° at locations 1, 2, and 3, respectively. The width of road (highway) was kept 7 m in the simulation. Afterwards, the slope material properties were assigned to these sections, and the bedrock lithology was taken for the inclined slopes, whereas asphalt material's property was assigned to the road. The bedrock lithology can be categorized by its characteristic normal restitution coefficient (0.35 ± 0.04), tangential restitution coefficient (0.85 ± 0.04), dynamic friction (0.5 ± 0.04), rolling friction (0.15 ± 0.02), and friction angle (30 ± 2)°. Furthermore, the asphalt (road) material has a normal restitution coefficient of 0.4 ± 0.04 and tangential restitution coefficient of 0.9 ± 0.03. The source (seeder) of the rockfall was the topmost point of the inclined slopes, with an initial horizontal velocity of 0.5 ± 0.1 m/s, while initial vertical and rotational velocity were kept 0 m/s. The rigid masses of 10 blocks were allowed to fall in each simulation, and outcomes were enumerated using the Monte-Carlo probabilistic numerical method. In each case, initially, the blocks fall on the slope-road boundary and bounce across the road.

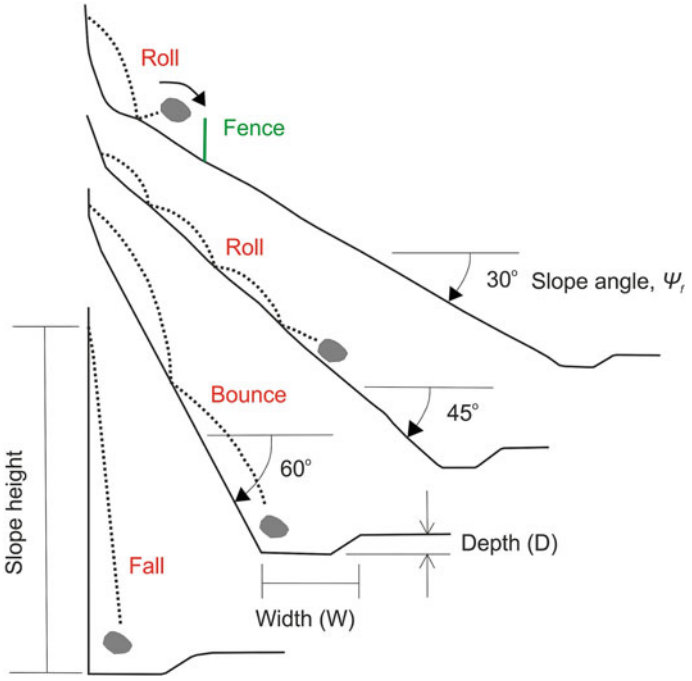

Fig. 4.4 Control of slope angle on the mode of rockfall (modified after Bar et al. 2016)

4.4 Results

The present analysis found that, for location 1, planar failure (with no limits) has a probability of 33.3% (Fig. 4.5a). The adjustment rating for the planar failure has been enumerated to calculate continuous slope mass rating (CSMR) for this site. This mode of sliding can be attributed to joint set 3 (Table 4.1), dipping 60° towards 250°. Additionally, the orientation factor (O-factor) for the analysis of J_r/J_a ratio in case of Q-slope will be ascertained for the planar failure (with no limits) along the same joint-set.

A similar analysis was done for location 2 (Fig. 4.5b), where the probability of wedge failure was affirmed along the intersection of joint sets J_2–J_3 (Table 4.1). One can either adopt planar or toppling failures to examine the adjustment rating. In this location, no such sliding was confirmed in the kinematic analysis. Hence, to decide the adjustment ratings for ascertaining the Continuous-SMR, one can assume the case of planar failure (without limits), as it has a slightly greater possibility than toppling with little change in geometry of either joints or slope.

Hence, the joint dipping at 80° towards 210 is considered for evaluating the adjustment rating of slopes. Moreover, to acquire Q-slope analysis for the site, one will consider the case of wedge failure along the intersection of joint-sets J_2 (70° → 110°) and J_3 (80° → 210°) to evaluate the orientation factor for J_r/J_a ratios.

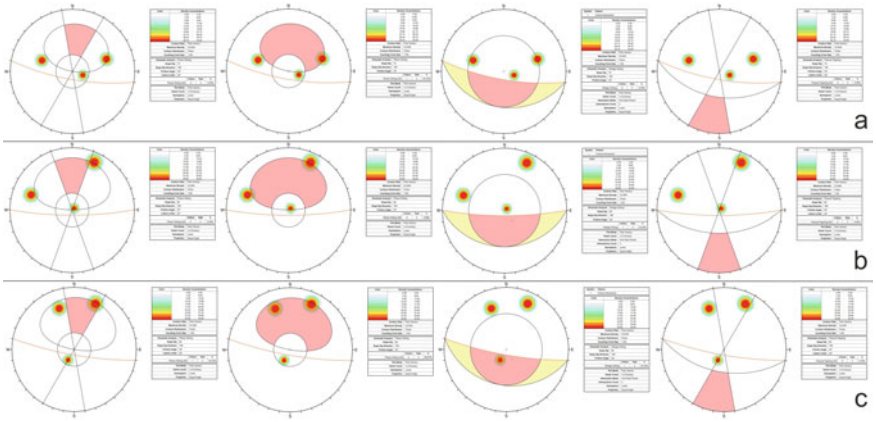

Fig. 4.5 Kinematic analysis at location 1 (a), location 2 (b), and location 3 (c)

Table 4.2 Point Load Strength Index (PLSI) for the samples collected in the study area

S.No.	Rock type	Thickness (mm)	Length (mm)	Width (mm)	Failure load (*N*)	PLSI (MPa)
1	Sandstone	42	59	85	24.5	7.50
2	Sandstone	72	43	80	37	7.81
3	Sandstone	40	80	90	16	4.87
4	Sandstone	55	74	78	27.5	7.34
5	Sandstone	47	78	74	22	7.01
Average PLSI						6.90

The outcomes of kinematic analysis of the slope at location 3 indicate that all the modes of failure are possible except toppling (Fig. 4.5c). The planar sliding, planar sliding (with no limits), and wedge sliding can occur with a probability of 33.3%, 66.6%, and 33.3%, respectively. Adjustment factor of SMR has been established considering the planar failure with the most critical joint set dipping 78° towards 205°. Furthermore, one will encompass wedge failure along the intersection of joint-sets J_1 (70° → 160) and J_3 (78° → 205) to get the orientation factor of J_r/J_a and perform the Q-slope analysis at the location 3. The laboratory examination of collected rock specimens concluded that the PLSI of the Dhandraul sandstone ranged between 4.87 to 7.81 MPa, indicating high strength samples (Table 4.2). Also, the UCS of these rocks had a median value of 138 MPa, on account of Eq. (4.3). The calculated RMR_{basic} values were 65, 62, and 67 for the locations 1, 2, and 3, respectively (Fig. 4.6). Similarly, the obtained values of continuous-SMR were 56, 52, and 32 for locations 1, 2, and 3, respectively, based on all the parameters accounted for in the present work (Table 4.3).

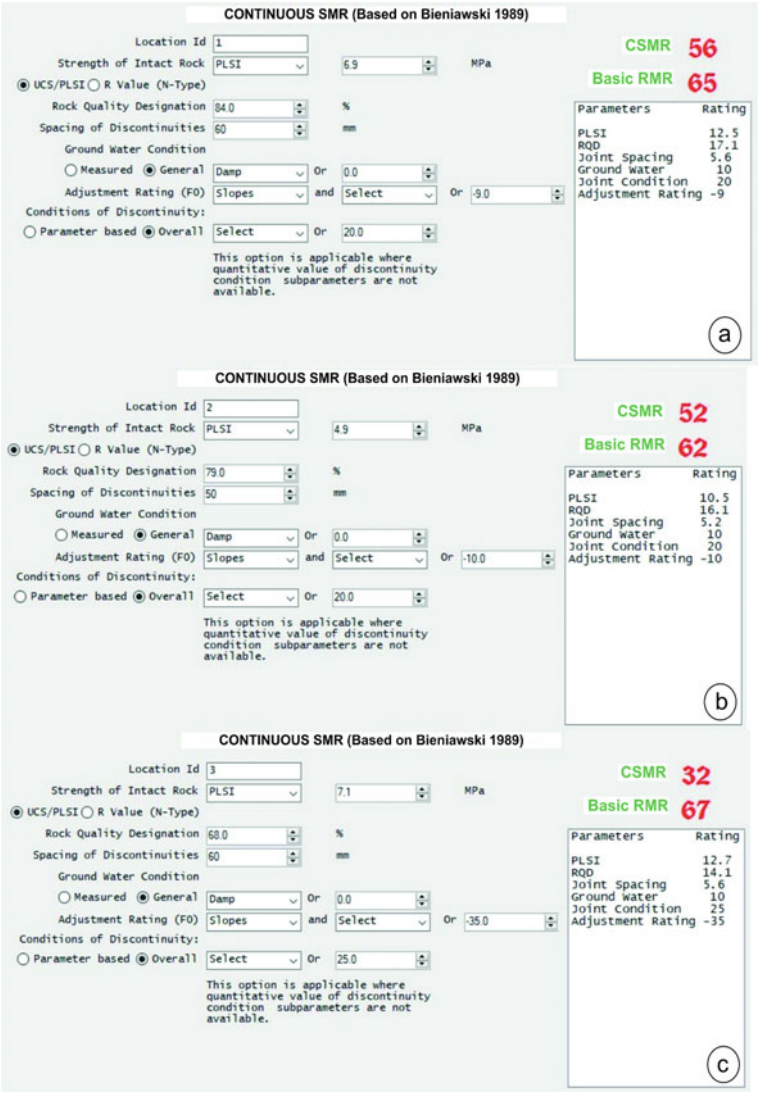

Fig. 4.6 Rock mass rating calculation using QuickRMR software for locations 1, 2, and 3

Apart from the CSMR, the Q-slope approach was incorporated into the study. Hence, a swift and scientific estimation of the maximum safe slope angles, without any heavy engineering accompaniments, can be made in the field. The present work acquired the following values of RQD, J_n, J_r, J_a, O-factor, J_w, and SRFslope through rigorous field investigation, kinematic analysis, and a short of arithmetic (Table 4.4).

For the investigated sections, the calculated values of the Q-slope range were 2.8, 4.21, and 5.44 for sites 1, 2 and 3, respectively. Therefore, the maximum slope angle

Table 4.3 Attributes of RMR_{basic} and CSMR, and their calculated values in the study area

Location	RQD (%)	PLSI (MPa)	Joint spacing (mm)	Joint condition	Ground-water condition	Adjustment rating	RMR_{basic}	CSMR
1	84	6.9	60	Slightly rough surfaces, separation <1 mm, highly weathered walls	Damp	– 9 ($F_1 = 0.15$; $F_2 = 1$; $F_3 = –60$; $F_4 = 0$)	65	56
2	79	4.87	50	Slightly rough surfaces, separation <1 mm, highly weathered walls	Damp	– 10 ($F_1 = 0.4$; $F_2 = 1$; $F_3 = –25$; $F_4 = 0$)	62	52
3	68	7.1	60	slightly rough surfaces, separation <1 mm, slightly weathered walls	Damp	– 35 ($F_1 = 0.7$; $F_2 = 1$; $F_3 = –50$; $F_4 = 0$)	67	32

Table 4.4 The deciding properties of Q-slope in the study area, and its' values (After, Bar and Barton 2017)

Q-slope parameters	Location 1	Location 2	Location 3
Kinematic Analysis	Planar sliding (with no-limits)	Wedge sliding along joint sets J_2 and J_3	Wedge sliding along joint sets J_1 and J_3
RQD	84%	79%	68%
J_n	Three joint sets	Three joint sets	Three joint sets
J_r	Rough or irregular plane	J_{r1}: Rough or irregular, undulating (for J_2) J_{r2}: Smooth, undulating (for J_3)	J_{r1}: Rough or irregular, undulating (for J_1) J_{r2}: Rough or irregular, undulating (for J_3)
J_a	Unaltered joint walls and surface staining only	J_{a1}: Unaltered joint wall and surface staining only (for J_2) J_{a2}: Unaltered joint wall and surface staining only (for J_3)	J_{a1}: Unaltered joint wall and surface staining only (for J_1) J_{a2}: Unaltered joint wall and surface staining only (for J_3)
O-factor	Quite favourable	O-factor (1): Very unfavourable (for J_2) O-factor (2): Very unfavourable (for J_3)	O-factor (1): Very unfavourable (for J_1) O-factor (2): Very unfavourable (for J_3)
J_{wice}	Stable-competent rocks lie in tropical storm	Stable-competent rocks lie in tropical storm	Stable-competent rocks lie in tropical storm
SRF_{Slope}	SRF_a: Slight loosening due to surface location, disturbance due to blasting or excavation SRF_b: $(\sigma_c/\sigma_1)^* = 171.42$ SRF_c: Not applicable	SRF_a: Slight loosening due to surface location, disturbance due to blasting or excavation SRF_b: $(\sigma_c/\sigma_1)^* = 170.43$ SRF_c: Not applicable	SRF_a: Slight loosening due to surface location, disturbance due to blasting or excavation SRF_b: $(\sigma_c/\sigma_1)^* = 246.95$ SRF_c: Not applicable
	Q-slope = 2.8 $\beta = 73.94°$	Q-slope = 4.21 $\beta = 77.40°$	Q-slope = 5.44 $\beta = 79.71°$

σ_c and σ_1 are the UCS and maximum principal stress; β is the maximum slope-angle stable without any heavy mechanical support (with 0.1% probability of failure)

that would be stable without installing any heavy engineering solutions is 73.94°, 77.40°, and 79.71°. Moreover, these estimated slope angles are 1° to 3° less than the actual cut-slope angle at these study sites. Hence, smaller localized failure cases may arise, which is evident in the study area as well. Several sandstone blocks of nearly rectangular to squared shapes were found scattered along the roadside during the field visit, as shown in Figs. 4.2, 4.3, and 4.4. Sudden loosening and fall of these blocks pose a major threat to the vehicles plying on the state highway-5A. On average, the blocks sizes were 1.266 × 1.266 × 1.266 m^3 in dimensions (2 m^3 in volume), with a dry density in the range 2,463 ± 266 kg/m^3 (Tenzer et al. 2011), with an equivalent weight of nearly 5,000 ± 500 kg.

Moreover, the rock blocks covered nearly one-fourth of the road at a few places, posing a considerable threat to the passing vehicles. The state highway is used by heavy vehicles like trucks, buses, and tractors to transport sand, sandstone, limestone, and other crucial goods. Even a tiny rockfall event can cause accidents, and also, a minor distraction while driving along these studied sites can lead to severe damage due to the collision with these existing detached rock blocks. Therefore, a scientific study of rockfall dynamics is necessary in the RocFall program (RocScience Inc. 2022). The detailed rockfall dynamics (like rockfall trajectory, bounce height, total kinetic energy, translational velocity, rotational velocity, and end-points) can be interpreted through Figs. 4.7, and 4.8 for each research area.

The rockfall examination at site 1 indicates a maximum total kinetic energy (TKE) of 1,550 ± 50 kJ, and the mean TKE is 1,200 ± 50 kJ at the slope-road boundary. Moreover, the TKE is reduced as blocks move further across the road, and finally, 70% of blocks come to rest just before crossing the road, while the rest, 30%, were stopped closer to the slope-road boundary. Additionally, the blocks attain an average height of 3 m, while the maximum height can reach 6 m across the road. The mean translational and rotational velocity of the falling blocks may vary in the range of 6–22 m/s and 1–7 rad/s, respectively, across the road. Similarly, at location 2, mean TKE

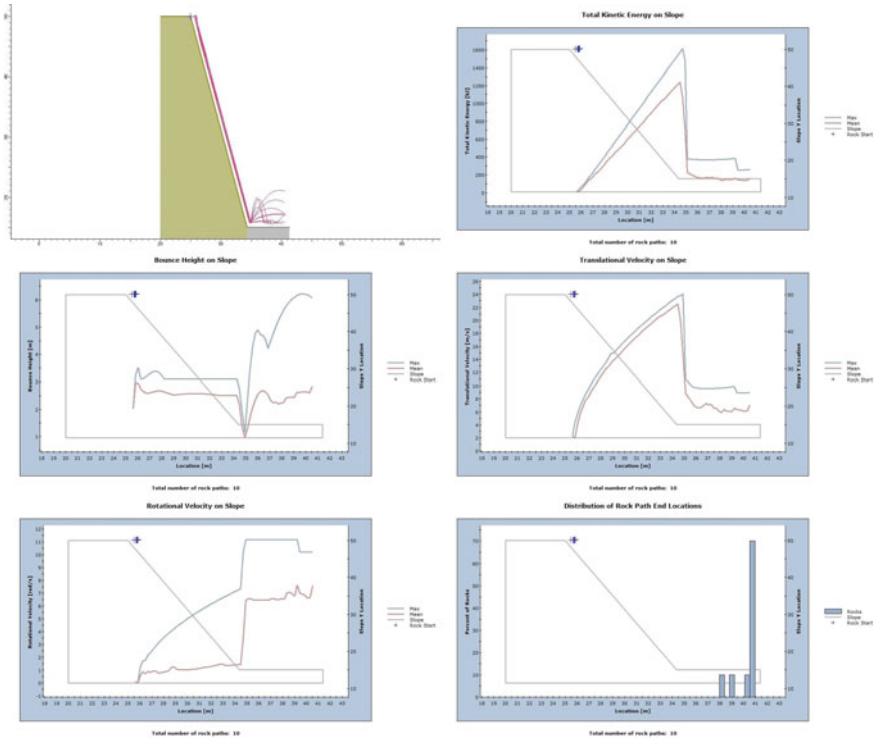

Fig. 4.7 Outcome of rockfall analysis at location 1

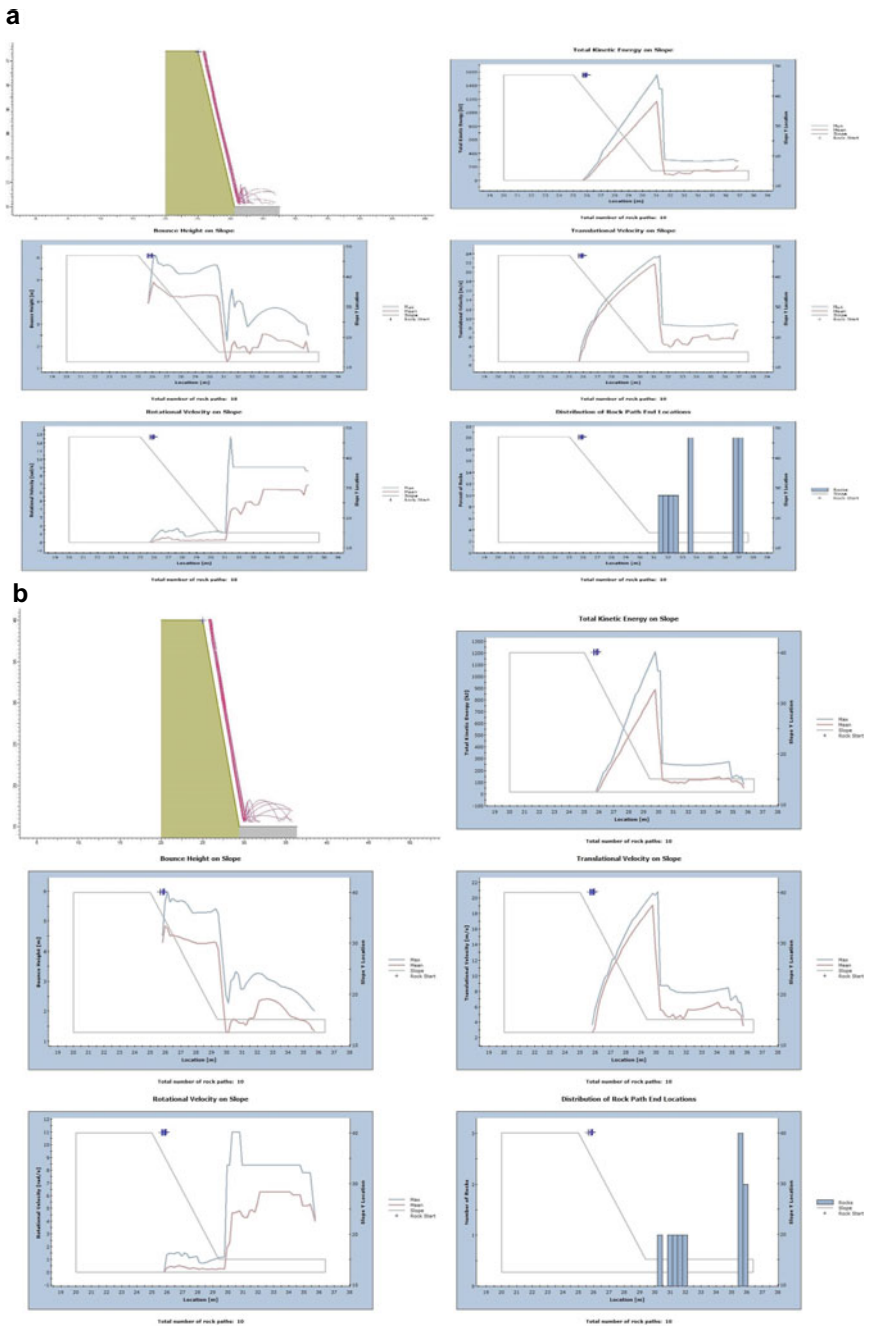

Fig. 4.8 Outcome of rockfall analysis at **(a)** locations 2 and **(b)** location 3

varies in the ranges of 100–1,100 kJ, while the mean bounce height achieved was in the range of 1.5–4 m across the road. The distribution of rock-path end locations reveals that approximately 40% of blocks were stopped within 2 m from the slope's toe, and 40% were stopped before 1 m at the other end of the road. Moreover, the simulated translation and rotational velocity of detached blocks were high and indicated rockfall danger. Furthermore, a detached block from the seeder at site 3 of the study area may bounce as high as 5 m and simultaneously gain a maximum TKE of 1,200 kJ. Approximately 50% of the blocks cross the road, and the rest 50% remained within 2 m from the slope-road boundary. Also, the mean translational velocity varies between 4 and 19 m/s, and mean rotational velocity ranges within 0–6 rad/s across the road.

4.5 Discussion

In this study, three sections have been investigated to assess the overall stability and in particular rockfall instability, in the upper reaches of Markundi hills, along state-highway-5, UP (India). Rock mass along the excavated slopes was blocky with three sets of prominent joints, plus a few random joints. The RQD values for three sections adapting scanline survey in the field were affirmed to be 84, 79 and 68 for the sites 1, 2, and 3, respectively. Due to the contrast in the joint condition, orientation, and hydrological conditions, the corresponding RMR_{basic}, CSMR, Q-slope, and rockfall simulation results vary at these locations. The kinematic analysis also demonstrated the possibility of planar failure in location-1 and wedge failure in locations 2 and 3. A previous study for kinematic and empirical assessment was conducted for two stretches of the hill slopes (Kumar et al. 2019). The ascribed RMR values in the present research work are in a similar range as in work done by Kumar et al (2019), through some RMR and SMR values given by them are lower range. As per Q-slope analysis, the excavated slopes were slightly steeper than the values recommended for reinforcement-free stable slopes. Thus, though the slopes are globally stable, it shows a propensity toward localized failures. Therefore, rockfall analysis was conducted to ascertain the rockfall trajectory, bounce height, total kinetic energy, translational velocity, rotational velocity, and end-points for all the locations. The possibility of rockfall events, irrespective of the failed blocks' size, is a critical factor in deciding the safety of a roadway. These parameters are crucial for designing mitigation measures in the studied section.

A median uniaxial compressive strength value of 138 MPa is incorporated to estimate CSMR and Q-slope based on laboratory testing. For location 1, kinematic analysis confirmed the case of planar failure (with no limits). This failure mode becomes the basis of adjustment rating and O-factor in a further empirical study. The RMR_{basic} and CSMR values determined for the site are 65 and 56, respectively, as the adjustment rating for the continuous slope mass rating is –9. Additionally, the study about Q-slope value 2.8 shows that the maximum slope angle at location-1 is 73.34°, without installing any sophisticated protection works. Also, the rockfall simulation

performed for the site reveals that the average total kinetic energy is ~1,200 kJ at the slope-road boundary. Most of the motion taken by detached blocks is of "fall" type until their first collision with the road surface. The maximum mean bounce height for the blocks are ~ 3 m, whereas the range of mean translational velocities is 6–22 m/s. In the same way, the tools and techniques employed at site-2 led to the understanding of slope safety concerns and ensuing better design. In this line of work, the slope was marked critical to wedge failure, but planar failure may occur with any unfavourable change in slope direction. So, the criteria of O-factor in the case of Q-slope considers the wedge instability condition, whereas the CSMR adopts the concepts of planar mode. The study shows the RMR_{basic} was designated a value of 62 at the second location, and owing to the adjustment rating (−10) the CSMR value was ascribed as 52 in the QuickRMR tool. Furthermore, the Q-slope study indicates that the steepest, safe, and engineering-free slope for location-2 should have an angle of 77.40° (~3° less than the present slope inclination). Additionally, the rockfall simulations at location 2 yielded a bounce height of 1.5–4 m, with a mean translational velocity of 4–21 m/s and a mean rotational velocity of 0–7 rad/m.

In-depth analysis for location-3 demonstrated a possibility of planar failure, planar failure (with no lateral limits), and wedge failure. RMRbasic value of 67 was designated for the slope, and while considering the contributing factors, the CSMR values calculated was 32, rendering it unstable. The safe slope angle for this slope section was 79.71°, quite close to the present slope angle, for the corresponding Q-slope value of 5.44. The rockfall analysis for this site assessed the mean total kinetic energy of the falling blocks to be 160–850 kJ, while the mean bounce height was 0.5–4.5 m. Also, the mean translational velocity of 4–19 m/s and rotational velocity of 0–6 m/s were calculated for this site. It can be seen that CSMR and Q-slope are not directly correlated and thus provide different information. Thus, it is judicious to use different approaches together for slope stability assessment to get a holistic examination.

4.6 Conclusion

Four distinct approaches were used for the analysis of 3 locations at state highway-5, Markundi hills. It is quite clear from the study that the approaches have both their utility and limitations. While kinematic analysis can demonstrate the possible failure mode, CSMR can be used to ascertain overall slope health in conjunction with kinematic analysis. Further, Q-slope is useful for finding the safe slope angle for a given rock mass and rockfall simulation tools are a great aid in calculating the bounce height and kinetic energy, which are used to design rockfall barriers and other protection measures. Analysis indicates that the studied slopes are under threat of rockfall hazards and need immediate installation of protection measures according to rockfall dynamics, as presented in this work. Additionally, the two-dimensional simulation of rockfall indicates that the construction of ditches and trenches near the slope-road boundary can reduce the risk to a greater extent. However, the ditches and trenches should provide the way for draining water. Otherwise, it may increase pore

water pressure, and eventually, slope failure can occur. It is also recommended to achieve the stability, to flatten the slopes at locations 1 and 2 by 2 and 3, respectively.

Acknowledgements Author AK is thankful to the BHU-IOE seed grant fund for the financial support. The authors are also grateful to Rocscience Inc., Canada, for the simulation suite.

References

Ansari T, Kainthola A, Singh KH, Singh TN, Sazid M (2021) Geotechnical and microstructural characteristics of phyllite derived soil; implications for slope stability, lesser Himalaya, Uttarakhand, India. Catena 196:104906

Auden JB (1933) Vindhyan sedimentation in the Son Valley, Mirzapur district. Mem Geol Surv India 62(2):141–250

Bar N, Barton N (2017) The Q-slope method for rock slope engineering. Rock Mech Rock Eng 50:3307–3322. https://doi.org/10.1007/s00603-017-1305-0

Bar N, Nicoll S, Pothitos F (2016) Rock fall trajectory field testing, model simulations and considerations for steep slope design in hard rock. In: Dight PM (ed) APSSIM 2016: proceedings of the first asia pacific slope stability in mining conference. Australian Centre for Geomechanics, Perth, pp 457–466. https://doi.org/10.36487/ACG_rep/1604_29_Bar

Barton N, Bar N (2015) Introducing the Q-slope method and its intended use within civil and mining engineering projects. In: Schubert W, Kluckner A (eds) Future development of rock mechanics; Proceedings of the ISRM regional symposium, Eurock 2015 and 64th geomechanics colloquium, Salzburg, 7–10 Oct 2015, pp 157–162

Barton N, Grimstad E (2014) Forty years with the Q-system in Norway and abroad, vol 4.1–4.25. Fjellsprengningsteknikk, Bergmekanikk, Geoteknikk, NFF, Oslo.

Basahel H, Mitri H (2017) Application of rock mass classification systems to rock slope stability assessment: a case study. J Rock Mech Geotech Eng 9(6):993–1009. https://doi.org/10.1016/j.jrmge.2017.07.007

Bhattacharya D, Joshi GB, Sharma GS, Sen DB (2008) A note on the uranium mineralisation along Jamual-Markundi fault, Sonbhadra and Sidhi districts, Uttar Pradesh and Madhya Pradesh. J Geol Soc India 71(1):125–128

Bieniawski ZT (1989) Engineering rock mass classification: a complete manual for engineers and geologists in mining, civil and petroleum engineering. John Wiley and Sons, New York

Castelli M, Scavia C, Bonnard C, Laloui L (2009) Mechanics and velocity of large landslides. Eng Geol 1(109):1–4

Castelli M, Torsello G, Vallero G (2021) Preliminary modeling of rockfall runout: definition of the input parameters for the QGIS plugin QPROTO. Geosciences 11(2):88

Census of India (2011) https://censusindia.gov.in/pca/cdb_pca_census/Houselisting-housing-UP.html. Accessed 29 Apr 2022

Deng X, Xu D, Zeng M, Qi Y (2018) Landslides and cropland abandonment in China's mountainous areas: spatial distribution, empirical analysis and policy implications. Sustainability 10(11):3909

Dikshit A, Sarkar R, Pradhan B, Segoni S, Alamri AM (2020) Rainfall induced landslide studies in Indian Himalayan region: a critical review. Appl Sci 10(7):2466

Financial Express (2022) https://www.financialexpress.com/events/national-road-infra-conclave-2022, Accessed 7 Feb 2022

Glade T (2003) Landslide occurrence as a response to land use change: a review of evidence from New Zealand. CATENA 51(3–4):297–314

Glade T, Crozier M, Smith P (2000) Applying probability determination to refine landslide-triggering rainfall thresholds using an empirical "Antecedent Daily Rainfall Model." Pure Appl Geophys 157(6):1059–1079

Glade T, Anderson MG, Crozier MJ (eds) (2006) Landslide hazard and risk. Wiley, New York

Guhathakurta P, Sudeep BL, Menon P, Prasad AK, Sable ST, Advani SC (2020) Observed rainfall variability and changes over Uttar Pradesh State. Climate Research and Services, India Meteorological Department, Ministry of Earth Sciences Pune. https://imdpune.gov.in/hydrology/rainfall%20variability%20page/uttar_final.pdf. Accessed on 29 Apr 2022

Hudson JA, Harrison JP (2000) Engineering rock mechanics. An introduction to principles, Elsevier Science Ltd., Oxford

Infante D, Martire D, Calcaterra D, Miele P, Scotto D, Santolo A, Ramondini M (2019) Integrated procedure for monitoring and assessment of linear infrastructures safety (I-Pro MONALISA) affected by slope instability. Appl Sci 9(24):5535. https://doi.org/10.3390/app9245535.

Kainthola A, Verma D, Thareja R, Singh TN (2013) A review on numerical slope stability analysis. Int J Sci Eng Technol Res 2(6):1315–1320

Kainthola A, Sharma V, Pandey VH, Jayal T, Singh M, Srivastav A, Singh PK, Champati PK, Singh TN (2021) Hill slope stability examination along Lower Tons valley, Garhwal Himalayas, India. Geomat Nat Haz Risk 12(1):900–921. https://doi.org/10.1080/19475705.2021.1906758

Kos A, Amann F, Strozzi T, Delaloye R, Von Ruette J, Springman S (2016) Contemporary glacier retreat triggers a rapid landslide response, Great Aletsch Glacier, Switzerland. Geophys Res Lett 43(24):12–466

Krishnan MS, Swaminath J (1959) The Great Vindhyan Basin of northern India. J Geol Soc India 1:10–30

Kumar B, Sharma SD, Sreenivas B, Dayal AM, Rao MN, Dubey N, Chawla BR (2002) Carbon, oxygen and strontium isotope geochemistry of proterozoic carbonate rocks of the Vindhyan Basin, central India. Precambr Res 113(1–2):43–63

Kumar S, Pandey HK, Singh PK, Venkatesha K (2019) Demarcation of probable failure zones based on SMR and kinematic analysis. Geomat Nat Haz Risk 10(1):1793–1804

Kumar S, Mishra AN, Singh AK, Mishra SR, Shahi AK (2020) Studies on the climatic variability analysis of Vindhyan Zone District Sonbhadra of Eastern Uttar Pradesh.

Kundu J, Sarkar K, Singh AK, Singh TN (2020) QuickRMR beta. A rock mass rating calculator based on continuous functions. https://jkundu.com/quickrmr. Accessed 2 Mar 2022

Kundu J, Sarkar K, Verma AK, Singh TN (2022) Novel methods for quantitative analysis of kinematic stability and slope mass rating in jointed rock slopes with the aid of a new computer application. Bull Eng Geol Env 81(1):1–9

Li D, Wong LNY (2013) Point load test on meta-sedimentary rocks and correlation to UCS and BTS. Rock Mech Rock Eng 46:889–896. https://doi.org/10.1007/s00603-012-0299-x

Mahanta B, Singh HO, Singh PK, Kainthola A, Singh TN (2016) Stability analysis of potential failure zones along NH-305, India. Nat Hazards 83(3):1341–1357

Mishra M, Sen S (2011) Geochemical signature for the grain size variation in the siliciclastics of the Kaimur Group, Vindhyan Supergroup from Markundi Ghat, Sonbhadra district, (U.P.), India. Geochem Int 49(3):290–305. https://doi.org/10.1134/S0016702911010071

Mishra M, Sen S (2012) Provenance, tectonic setting and source-area weathering of Mesoproterozoic Kaimur Group, Vindhyan Supergroup, Central India. Geol Acta 10(3):283–293. https://doi.org/10.1007/s11631-010-0021-1

NDMA (2022) https://ndma.gov.in/Natural-Hazards/Landslide. Accessed 01 Mar 2022

NDR (2022) https://www.ndrdgh.gov.in/NDR/?page_id=831&page_id=831. Accessed 29 Apr 2022

Petley DN, Dunning SA, Rosser NJ, Hungr O (2005) The analysis of global landslide risk through the creation of a database of worldwide landslide fatalities. Landslide Risk Manag 52:367–373

Prakash C, Agarwal KK, Sharma VK (2015) Structural control of landslides in Eastern Kumaun Himalaya: case study from Sukhidhang—Ladhiya section. J Geol Soc India 86(5):507–512

Priest SD, Hudson J (1976) Discontinuity spacing in rock. Int J Rock Mech Min Sci Geomech Abstr 13(5):135–148

Quasim MA, Ahmad AH, Sachan HK, Ghosh SK (2019) Recrystallization and provenance history of the upper Kaimur Group siliciclastics, Son Valley, India: coupled petrographic and fluid inclusion proxy. J Geol Soc India 93(2):177–184. https://doi.org/10.1007/s12594-019-1148-2

Ray A, Kumar V, Kumar A, Rai R, Khandelwal M, Singh TN (2020) Stability prediction of Himalayan residual soil slope using artificial neural network. Nat Hazards 103(3):3523–3540

RocScience Inc (2022) A bundle of 2D and 3D geotechnical tools. https://www.rocscience.com/

Romana M (1985) New adjustment ratings for application of Bieniawski classification to slopes. In: Proceedings of the international symposium on the role of rock mechanics. ISRM, Zacatecas, pp 49–53

Scavia C, Barbero M, Castelli M, Marchelli M, Peila D, Torsello G, Vallero G (2020) Evaluating rockfall risk: some critical aspects. Geosciences 10(3):98

Singh TN, Verma AK, Sarkar K (2010) Static and dynamic analysis of a landslide. Geomat Nat Haz Risk 1(4):323–338

Singh TN, Kainthola A, Venkatesh A (2012) Correlation between point load index and uniaxial compressive strength for different rock types. Rock Mech Rock Eng 45(2):259–264

Singh PK, Wasnik AB, Kainthola A, Sazid M, Singh TN (2013) The stability of road cut cliff face along SH-121: a case study. Nat Hazards 68(2):497–507

Singh PK, Kainthola A, Panthee S, Singh TN (2016) Rockfall analysis along transportation corridors in high hill slopes. Environ Earth Sci 75(5):1–1

Singh PK, Singh KK, Singh TN (2017) Slope failure in stratified rocks: a case from NE Himalaya, India. Landslides 14(4):1319–1331

Singh AK, Kundu J, Sarkar K (2018) Stability analysis of a recurring soil slope failure along NH-5, Himachal Himalaya, India. Nat Hazards 90(2):863–885

Singh HO, Ansari TA, Singh TN, Singh KH (2020) Analytical and numerical stability analysis of road cut slopes in Garhwal Himalaya, India. Geotech Geol Eng 38(5):4811–4829

Tenzer R, Sirguey P, Rattenbury M, Nicolson J (2011) A digital rock density map of New Zealand. Comput Geosci 37(8):1181–1191

Tiwari VN, Pandey VHR, Kainthola A, Singh PK, Singh KH, Singh TN (2020) Assessment of Karmi Landslide Zone, Bageshwar, Uttarakhand, India. J Geol Soc India 96(4):385–393. https://doi.org/10.1007/s12594-020-1567-0

Tripathy GR, Singh SK (2015) Re-Os depositional age for black shales from the Kaimur Group, Upper Vindhyan, India. Chem Geol 413:63–72. https://doi.org/10.1016/j.chemgeo.2015.08.011

Wei L, Hu K, Hu X, Wu C, Zhang X (2022) Quantitative multi-hazard risk assessment to buildings in the Jiuzhaigou valley, a world natural heritage site in Western China. Geomat Nat Haz Risk 13(1):193–221. https://doi.org/10.1080/19475705.2021.2004244

Yoon WS, Jeong UJ, Kim JH (2002) Kinematic analysis for sliding failure of multi-faced rock slopes. Eng Geol 67(1–2):51–61

Zhou X, Qian Q, Cheng H, Zhang H (2015) Stability analysis of two-dimensional landslides subjected to seismic loads. Acta Mech Solida Sin 28(3):262–276